CORTEX 48 (2012) 1298–1309

Available online at www.sciencedirect.com

SciVerse ScienceDirect

Journal homepage: www.elsevier.com/locate/cortex

Research report

Brain networks in posterior cortical atrophy: A single case tractography study and literature review

Raffaella Migliaccio [a,b], Federica Agosta [d], Monica N. Toba [a], Dalila Samri [a], Fabian Corlier [a], Leonardo C. de Souza [a], Marie Chupin [a,f], Michael Sharman [a,c], Maria L. Gorno-Tempini [e], Bruno Dubois [a], Massimo Filippi [d] and Paolo Bartolomeo [a,b,*]

[a] Inserm-UPMC UMRS 975, CR-ICM, Centre de Recherche de l'Institut du Cerveau et de la Moelle épinière, Hôpital de la Pitié-Salpêtrière, Paris, France
[b] Department of Psychology, Catholic University, Milan, Italy
[c] CENIR, Centre de Neuroimagerie de Recherche, Paris, France
[d] Neuroimaging Research Unit, INSPE, Division of Neuroscience, Scientific Institute and University Ospedale San Raffaele, Milan, Italy
[e] Memory and Aging Center, Department of Neurology, UCSF, San Francisco, CA, USA
[f] CNRS, UMR-S7225, Paris, France

ARTICLE INFO

Article history:
Received 8 March 2011
Reviewed 21 March 2011
Revised 1 April 2011
Accepted 5 October 2011
Action editor Sergio Della Sala
Published online 20 October 2011

Keywords:
Brain networks
Visuo-spatial attention
Optic ataxia
Ideomotor apraxia
Neurodegeneration

ABSTRACT

Posterior cortical atrophy (PCA) is rare neurodegenerative dementia, clinically characterized by a progressive decline in higher-visual object and space processing. After a brief review of the literature on the neuroimaging in PCA, here we present a study of the brain structural connectivity in a patient with PCA and progressive isolated visual and visuo-motor signs. Clinical and cognitive data were acquired in a 58-years-old patient (woman, right-handed, disease duration 18 months). Brain structural and diffusion tensor (DT) Magnetic Resonance Imaging (MRI) were obtained. A voxel-based morphometry (VBM) study was performed to explore the pattern of gray matter (GM) atrophy, and a fully automatic segmentation was assessed to obtain the hippocampal volumes. DT MRI-based tractography was used to assess the integrity of long-range white matter (WM) pathways in the patient and in six sex- and age-matched healthy subjects. This PCA patient had a clinical syndrome characterized by left visual neglect, optic ataxia, and left limb apraxia, as well as mild visuo-spatial episodic memory impairment. VBM study showed bilateral posterior GM atrophy with right predominance; DT MRI tractography demonstrated WM damage to the right hemisphere only, including the superior and inferior longitudinal fasciculi and the inferior fronto-occipital fasciculus, as compared to age-matched controls. The homologous left-hemisphere tracts were spared. No difference was found between left and right hippocampal volumes. These data suggest that selective visuo-spatial deficits typical of PCA might not result from cortical damage alone, but by a right-lateralized network-level dysfunction including WM damage along the major visual pathways.

* *Corresponding author*. INSERM UMRS 975 ICM, Institut du Cerveau et de la Moelle épinière, Hôpital de la Pitié-Salpêtrière, 47 Bd de l'Hôpital, 75651 Paris, Cedex 13, France.
E-mail address: paolo.bartolomeo@upmc.fr (P. Bartolomeo).
0010-9452/$ – see front matter © 2011 Elsevier Srl. All rights reserved.
doi:10.1016/j.cortex.2011.10.002

1. Introduction

1.1. The neuroanatomy of posterior cortical atrophy (PCA)

PCA is a rare, early-onset (usually before 65 years) neurodegenerative dementia, characterized by initially isolated, progressive impairment of higher order visual and visuo-spatial skills, which usually manifest as visual agnosia, prosopagnosia, environmental disorientation, elements of Balint's syndrome and visual neglect (Andrade et al., 2010). While these deficits are hallmark features of the clinical syndrome, at presentation to specialized clinics, they can often be accompanied by deficits in praxis and language (e.g., dressing apraxia, transcortical sensory aphasia, and alexia) (Benson et al., 1988; Freedman et al., 1991; Mendez et al., 2002; Tang-Wai et al., 2004; McMonagle et al., 2006). Consistent with their clinical presentation, patients with PCA show gray matter (GM) loss in parieto-occipital and posterior temporal cortices, which is often more prominent in the right hemisphere (Galton et al., 2000; Whitwell et al., 2007). Positron emission topography (PET) studies have reported a prominent hypometabolism in the same posterior brain areas (Nestor et al., 2003; Schmidtke et al., 2005; Bokde et al., 2005). Although PCA patients do not meet clinical criteria for Alzheimer's disease (AD), because of the lack of memory impairment as core of the syndrome, pathological series have found that the majority of PCA patients have senile plaques and neurofibrillary tangles, both hallmarks of AD, at autopsy (von Gunten et al., 2006; Renner et al., 2004; Tang-Wai et al., 2004; Alladi et al., 2007). In a recent study comparing clinical, biological and anatomical evidence between PCA and early-onset AD (age $<$ 65) was directly performed (Migliaccio et al., 2009), voxel-based morphometry (VBM) results demonstrated a large region of overlapping atrophy between PCA and early-onset AD in the temporo-parietal regions. These regions are known to be preferentially affected in AD pathologically, structurally, and functionally, especially in younger patients (Yasuno et al., 1998; Frisoni et al., 2007; Rabinovici et al., 2010). Migliaccio et al. proposed that although location of atrophy is not an absolute marker of pathology, it does increase the probability of specific underlying pathologic processes, because different brain regions seem to be more vulnerable to specific diseases (Seeley et al., 2009). For these reasons and because of the early age at presentation ($<$65 years), the definition of "nontypical form of AD with an early age of onset" has been proposed for PCA (Migliaccio et al., 2009).

In PCA, the distribution of AD pathological changes is preponderant in occipital, parietal, and middle/inferior temporal cortices at the autopsy [see (von Gunten et al., 2006) for review]. However, recent studies conducted *in vivo*, using PET with [11C]-labeled Pittsburgh compound-B (Rosenbloom et al., 2011; de Souza et al., 2011), found no difference in the topography of fibrillar amyloid-β deposition between typical AD and PCA, and concluded that brain damage in PCA was not explained by the distribution of amyloid; if so, amyloid would not be the critical pathological change driving neurodegeneration in PCA.

White matter (WM) damage has attracted less interest. To date, only two single case studies (Yoshida et al., 2004; Duning et al., 2009) have assessed WM integrity in PCA by using diffusion tensor (DT) Magnetic Resonance Imaging (MRI) and a region of interest (ROI)-based approach. In one study (Duning et al., 2009), cognitive deterioration (over a period of 15 months) was associated with diffusivity changes of the occipito-parietal WM, rather than with overall GM and WM atrophy progression. In the other study (Yoshida et al., 2004), decreased fractional anisotropy (FA) was detected in the splenium of the corpus callosum (CC), possibly reflecting neuronal loss in caudal brain regions.

The lesional basis of PCA is not fully defined yet. Recent Single-photon emission computed tomography (SPECT) studies indicate a direct correlation between left inferior parietal hypoperfusion and acalculia, elements of Gerstmann's syndrome, left–right disorientation and limb apraxia scores, whereas damage to the bilateral dorsal occipito-parietal regions appeared to be involved in Balint's syndrome (Kas et al., 2011). In another study, structural MRI demonstrated a tendency toward a decreased cortical thickness in occipito-temporal and occipito-parietal cortices in PCA patients with predominant visuo-perceptual and visuo-spatial deficits, respectively (Lehmann et al., 2011). These results are consistent with the classical dichotomy between ventral (occipito-temporal) and dorsal (occipito-parietal) cortical visual streams (see Ungerleider and Mishkin, 1982).

It is to be noted, however, that the ventral–dorsal dichotomy may represent an oversimplification. Both the ventral and the dorsal streams are composed of several distinct pathways, which are starting to be defined both anatomically and functionally (Rizzolatti and Matelli, 2003; Schmahmann and Pandya, 2006; Kravitz et al., 2011; Thiebaut de Schotten et al., 2011). It is conceivable that different combinations of damage to these pathways give rise to distinct patterns of visual or visuo-motor impairment (Bartolomeo et al., 2007).

In neurodegenerative conditions, the prevalently cortical pathology usually inspires accounts of structure-function correlations based on strict cortical localization. Thus, neuropsychological deficits are conceived as resulting from cortical degeneration. However, in recent years a strict cortical localization approach for cognitive functions is changing toward more network-based hypotheses, according to which cognitive functions emerge from the interruption of the flow of information across large-scale networks linking different cortical regions (Catani and ffytche, 2005; Bartolomeo, 2011). The network-based approach contends that not only cortical lesions, but also damage to the WM connections between cortical areas can induce network dysfunction and, hence, cognitive disorders (Mesulam, 2009). On the other hand, WM abnormalities such as rarefaction, loss of axons, oligodendrocytes and reactive astrocytosis have also been reported in neurodegenerative conditions. However, it remains to be seen whether and to what extent damage to WM pathways can correlate with neuropsychological deficits.

A network approach to clinico-anatomical correlations seems particularly appropriate to degenerative disorders, in which neural damage does not distribute along vascular territories such as in stroke, but seem to follow neurofunctional systems implemented in large-scale brain networks. According to the network vulnerability target hypothesis, different networks show peculiar patterns of vulnerability in different neurodegenerative conditions (Seeley et al., 2009).

2. Case report

The present case report aims at exploring these open issues by taking advantage of detailed neuropsychological and neuroimaging studies, including DT MRI-based tractography of long-range WM tracts, which permits to explore microscopic changes undetected when using conventional MRI. Once specific tracts were identified, values of fiber integrity were obtained, such as mean diffusivity (MD), FA, parallel ($\lambda_{//}$) and transverse ($\lambda_{\perp}$) diffusivities. These metrics have the potential to elucidate the possible substrates of WM damage (Pierpaoli et al., 2001).

A 58-year-old woman, medical doctor, with unremarkable prior medical history, reported multiple minor car accidents against left-sided obstacles during the previous 18 months. Clinical and neuropsychological examinations (Table 1) revealed signs of left visual neglect, optic ataxia and ocular apraxia, as well as left ideomotor apraxia. There was mild memory impairment, especially with visuo-spatial material, and a very mild simultanagnosia. Executive functions and calculation were relatively spared. Rare difficulties in word-finding and occasional phonologic paraphasias occurred. Fluctuating signs of tactile anomia for the left hand were also present. Cerebrospinal fluid (CSF) analysis revealed 188 tau-protein pg/ml (100–450 normal), P-tau 62 pg/ml (<60 normal), and beta-amyloid 263 pg/ml (500–1500 normal). High-resolution MRI demonstrated bilateral cortical atrophy mainly located in the parietal lobes (Fig. 1). In agreement with current clinical criteria, a diagnosis of PCA was made.

During a 2-year follow-up, the neuropsychological profile remained highly asymmetric with language and verbal memory largely preserved, while left visual neglect continued to represent the most severe symptom, and remained a substantial source of handicap in her everyday life.

2.1. *Neuropsychological study*

A detailed assessment of visuo-spatial attentional and visuo-motor deficits, as well as of ideomotor apraxia was conducted (Table 1, Figs. 2 and 3).

2.1.1. *Neglect assessment*

A paper-and-pencil battery (Azouvi et al., 2006) sensitive to signs of visual neglect was used. In addition, a tactile line bisection was performed by asking the patient to indicate the center of five paperboard lines (20 cm × 1 cm, i.e., the same length as the stimuli used for visual line bisection). Tactile and auditory extinctions were also evaluated.

2.1.2. *Optic ataxia*

Drawing on previous studies (for review see Pisella et al., 2008), we developed a computerized test adopting touch-screen technology to assess manual reaching in the visual periphery and to record spatio-temporal performances. A laptop computer, implemented with a touch-screen, at a distance of 50 cm from the subject, was used. The reaching task employed homemade software. The patient fixated a white cross on a black background (Fig. 3A) and had to

Table 1 – Cognitive assessment.

Test	Score (hits/max)
MMSE	23/30
Memory	
Verbal span direct	4
Verbal span indirect	4
Visual span direct	2*
Visual span indirect	0*
Verbal episodic memory – immediate	13/16
Verbal episodic memory – delay	40/48
Visual episodic memory – 12 images	1/6*
Rey figure recall	0/36*
Executive functions (FAB)	13/18
Language	
Naming	79/80
Fluency	Normal
Single-word repetition	10/10
Sentence repetition	15/16
Dictation of irregular words	46/50*
Dictation of pseudowords	10/10
Visuo-spatial abilities	
Rey figure copy	2/36*
Copy of figure	Impaired
Praxies – ideomotor apraxia	
Verbal commands	R: 9/12; L: 1/12*
Real objects	R: 12/12; L: 9/12*
Closed eyes	R: 10/12; L: 6/12*
Kinesthetic sensitivity	Normal
Tactile anomia	R = Normal; L = delay of the answer
Balint syndrome	Optic ataxia (see experiment)* Ocular apraxia (clinical evaluation: 2/4)* Simultanagnosia (overlapping figures test: 16/20)*
Gerstmann syndrome	Absent
Neglect battery (BEN)	
Visual double simultaneous stimulation	7/12*
Tactile double simultaneous stimulation	10/12
Auditory double simultaneous stimulation	9/9
Visual line bisection	19%* Rightward deviation
Tactile line bisection	25%* Rightward deviation
Ogden drawing copy	.5/4*
Clock drawing test	0/4*
Bells cancellation test	14/15

Scores indicate the number of correct responses out of the maximal score. Asterisks indicate pathological scores compared to normative data.
Abbreviations: BEN: Batterie d'Evaluation de la Négligence spatiale; FAB: Frontal Assessment Battery; L = left; MMSE: Mini Mental State Examination; R = right.

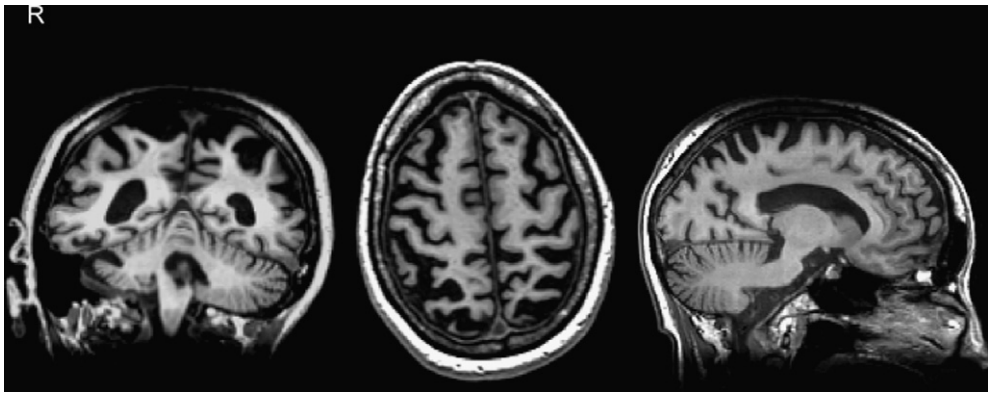

Fig. 1 – Native high-resolution structural MRI of the PCA patient. Note the bilateral posterior brain atrophy.

manually reach visual targets (white circles with a 2-cm diameter), appearing in pseudo-random locations on the touch-screen. Targets had to be touched by a stylus pen. The use of a pen provided the patient with the necessary precision to touch the relatively small targets, and prevented the occurrence of errors, such as touching the screen with the other fingers. Each test session includes 30 targets, presented every 4 sec. The spatial co-ordinates of each touch event were recorded. The patient performed the task by using the right arm; severe limb apraxia prevented her to use her left arm for this task.

2.1.3. *Ideomotor apraxia*

In addition to clinical apraxia assessment with verbal commands, we also tested the patient's ability to use real objects (Peigneux and Van der Linden, 2000). We also asked the patient to execute the same gestures in the absence of vision.

2.2. *Anatomical study*

MR images were acquired on a 3.0 T Siemens MRI system at the CENIR (Center for NeuroImaging Research – http://www.cenir.org/), Salpêtrière Hospital. For DT MRI, we employed single-shot spin-echo echo-planar images (EPI) with 50 directions ($b = 1000$ sec/mm^2, repetition time/echo time = 12,000 msec/80 msec; flip angle = 90°; field of view = 256 mm^2; matrix = 128 × 128; voxel size = 2 × 2 × 2 mm; slice thickness = 2 mm). Structural MRI sequences included double spin-echo sequence in order to exclude other causes of focal or diffuse brain damage, including extensive WM disease.

2.2.1. *Tractography study*

Fiber tracking was performed using Diffusion Toolkit based on the Interpolated streamline method, and TrackVis software (Wedeen et al., 2008). Fiber tracts were launched from every voxel in the brain and were terminated upon entering a voxel if the FA value was less than .15, or voxel-to-voxel deflection angle was larger than 45°. The fiber tracking software allows the identification of the tracts, visualization in 3D, and quantitative analyses on the delineated tracts. ROIs were defined manually on the axial, coronal, and sagittal FA images of each subject, and were used as seed regions for tracking. Based on previous tractography work (Catani and Thiebaut de Schotten, 2008) (Agosta et al., 2010), the trajectories of the inferior longitudinal fasciculus (ILF), inferior fronto-occipital fasciculus (IFOF), fronto-parietal superior longitudinal fasciculus (F-P SLF), and arcuate fasciculi, as well as the CC, were obtained in both hemispheres for the patient and six healthy age-matched right-handed women (mean age, 59.3 years; Montreal Cognitive Assessment – MOCA, mean score 28.7/30). ROIs were delineated as follows:

- *ILF ROIs*: a two-ROIs approach was used. The first ROI was drawn on axial FA slices around the WM of the anterior temporal lobe (ATL). The second ROI was defined on axial FA slices around the occipital WM lying posterior to the splenium of the CC. In order to include the entire occipital lobe, coronal and sagittal FA maps were used as reference to identify the parieto-occipital sulcus.
- *IFOF ROIs*: a two-ROIs approach was used. The first region was delineated around the occipital lobe using the same criteria used for the delineation of this occipital region for

Fig. 2 – From left to right: clock drawing test, copy of drawing, line bisection.

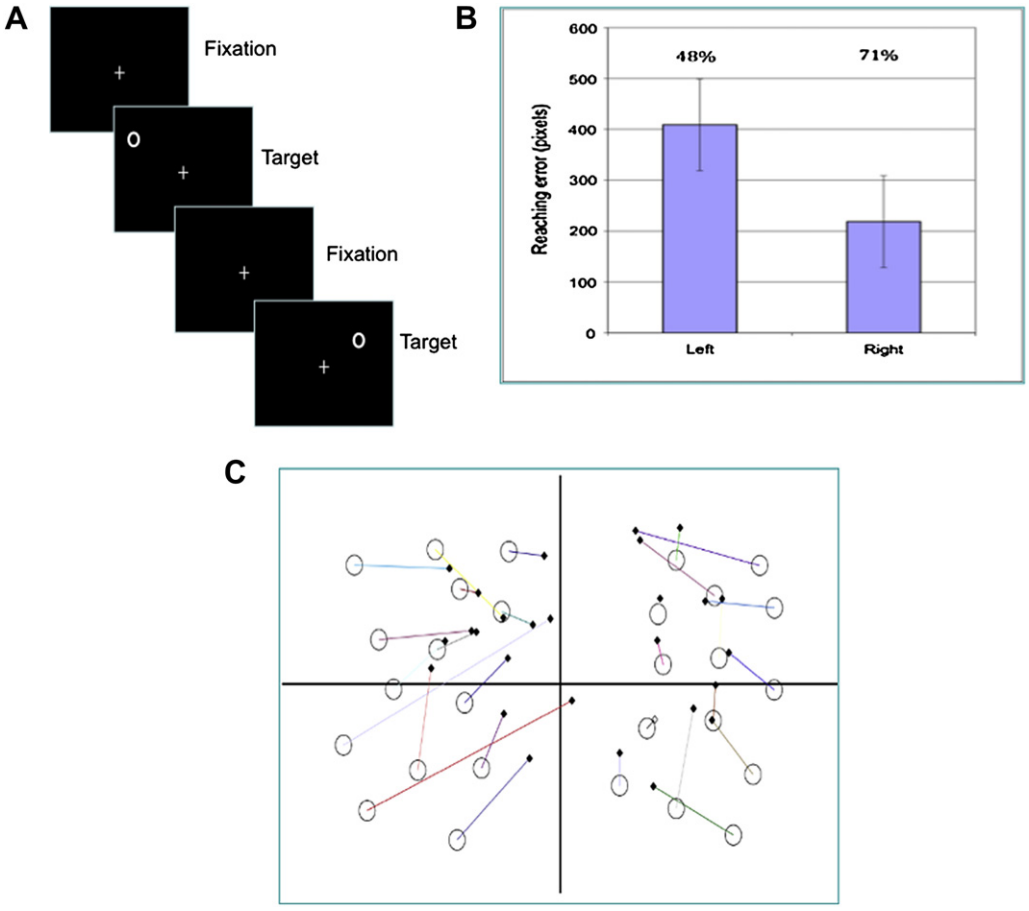

Fig. 3 – A) Optic ataxia experiment; B) Graphic showing the misreaching errors (in pixels) for left- and right-sided peripheral targets and the percentages of items that elicited a hand reaching movement; C) The circles represent the targets and the lines represent the directions of the errors.

the ILF. The second region is defined around the external/extreme capsule.

- *fronto-parietal SLF and arcuate fasciculus ROIs*: a single ROI was drawn on the axial slice of the color-coded map to define all of the fibers oriented in an anterior–posterior direction (green on the color maps), running lateral to the corona radiata and medial to the cortex. Because all the SLF bundles pass through this bottleneck, it is an ideal region to define the main body of the tract. All the tracts that did not reach the frontal lobe were removed since they represent erroneous tracts or real tracts not meeting our interest. Then, second ROI including temporal region was selected to obtain the arcuate fasciculus connecting frontal to temporal regions. Temporal ROIs were defined on sagittal FA slices around the entire descending portion of the SLF, corresponding approximately to the posterior third of the superior temporal gyrus, bordered caudally and dorsally by the angular and supramarginal gyri, respectively. We defined the rostral border of the temporal ROIs as the position of the Heschl's gyrus. The same ROI for the arcuate fasciculus was then used as exclusion ROI to isolate the fronto-parietal component of SLF.
- *CC ROIs*: a single ROI was defined around the CC on a midsagittal slice.

In order to avoid differences in the size of ROIs between the hemispheres in patient and controls, the volume (expressed in voxels) of each ROI was calculated and compared. ROIs volumes for the patient were: left occipital = 1242, right = 1226; left frontal external/extreme capsule = 243, right = 210; left anterior temporal = 3134, right = 3444; left parietal = 203, right = 180. Mean ROIs volumes (standard deviation – SD) for the control group were: left occipital = 2191 (642.3), right = 2244 (832.9); left frontal external/extreme capsule = 229 (89.1), right = 219 (80.7); left anterior temporal = 3149 (567), right = 3336 (739); left parietal = 165 (41.3), right = 168 (39.9). Paired *t*-tests showed no significant difference between right and left ROI volumes in the patient ($p = .53$) and control group (overall comparison: left occipital ROI *vs* right $p = .90$; left frontal external/extreme capsule ROI *vs* right $p = .84$; left anterior temporal ROI *vs* right $p = .63$; left parietal ROI *vs* right $p = .92$). Finally, there was no significant difference between right and left ROIs when comparing the patient to the control group (see Crawford and Garthwaite, 2002): left occipital ROI $p = .23$, right occipital ROI $p = .31$; left frontal external/extreme capsule ROI $p = .89$, right frontal external/extreme capsule ROI $p = .92$; left anterior temporal ROI $p = .98$, right anterior temporal ROI $p = .89$; left parietal ROI $p = .43$, right parietal ROI $p = .79$.

All tracts were successfully identified in all subjects, except for the right arcuate fasciculus, which was found only in two control subjects (see Catani et al., 2007), and was therefore excluded from the analysis. MD, FA, $\lambda_{//}$, and $\lambda_{\perp}$ were obtained for each tract, as well as the number of streamlines as a measure of tract volume.

2.2.2. VBM

VBM was used to investigate patterns of GM atrophy in the patient relative to a larger control group of 15 right-handed and age-matched healthy subjects (13 women; mean age: 60 years ± 2; MOCA, mean score 28.7/30). VBM was performed using Statistical Parametric Mapping (SPM8) and the Diffeomorphic Anatomical Registration Exponentiated Lie Algebra (DARTEL) registration method (Ashburner, 2007). Briefly, (i) T1-weighted images were segmented using VBM5.1 toolbox (http://dbm.neuro.uni-jena.de/beta-version-of-vbm51-toolbox/) to produce GM, WM and CSF probability maps in the Montreal Neurological Institute (MNI) space; (ii) original T1-weighted images were imported in DARTEL, (iii) rigidly aligned, (iv) segmented a second time (using the segmentation parameters from step [i]), and (v) resampled to 1.5 mm isotropic voxels; (vi) GM and WM segments were coregistered simultaneously using the fast diffeomorphic image registration algorithm; (vii) the flow fields were then applied to the rigidly aligned segments to warp them to the common DARTEL space and then modulated using the Jacobian determinants. Since the DARTEL process warps to a common space that is smaller than the MNI space, the modulated images from DARTEL were normalized to the MNI template using an affine transformation estimated from the DARTEL GM template and the a priori GM probability map without re-sampling (http://brainmap.wisc.edu/ normalize DARTEL to MNI). Finally, the images were smoothed with an 8-mm full-width at half-maximum Gaussian kernel. GM maps were compared between patient and controls using a two-sample *t*-test in SPM8. Age, gender, and total intracranial volume were used as confounding variables. We accepted a level of significance at $p < .05$ corrected for multiple comparisons (Table 3), because of the risk of false negatives in single subject analysis, we also report effects at $p < .001$ uncorrected (Fig. 1 and Table 3), as previously described (Gorno-Tempini et al., 2004).

2.2.3. Segmentation of the hippocampus

Hippocampal volumes were obtained by using a fully automatic segmentation (Chupin et al., 2009).

All participants provided written informed consent to participate in the study, which was approved by the local ethics committee.

3. Results

3.1. Neuropsychological study

The patient had moderate rightward deviation on both visual (19%) and tactile (25%) line bisection (Table 1), and pathological scores on landscape drawing copy (.5/4) and clock drawing test (0/4) (Fig. 2). Patient showed no auditory extinction (9/9), although she had some difficulty to identify auditory stimuli presented on the left side. There were rare left tactile extinctions on double stimulation (10/12).

Fig. 3 shows the setting of computerized assessment of optic ataxia (panel A) and the analysis of end-point errors (panels B and C). Fewer items elicited hand reaching movements in the left than in the right visual field (respectively, 48% and 71%), consistent with the presence of left neglect. Reaching errors were directed toward the fixation cross, in agreement with previous reports of so-called magnetic misreaching, where the reaching movements appear to be "locked" to the eye fixation point (Jackson et al., 2005). Detected left-sided targets elicited larger reaching errors than right-sided targets (Fig. 3B; mean difference, 166 pixels; *t*-test assuming unequal variances = 3.92, d.f. = 98, $p = .00017$, two-tailed).

Left-hand ideomotor apraxia was mainly characterized by spatial errors; performance improved with the use of real objects, and slightly deteriorated when the patient executed the movements with closed eyes (Table 1).

3.2. Tractography study

Statistical analysis of DT MRI-derived metrics was conducted by using significance test for comparing an individual case with small control samples (Crawford and Garthwaite, 2002). Differences between patient and controls were found in all right-hemisphere fasciculi. The patient had higher MD, $\lambda_{//}$ and $\lambda_{\perp}$ and lower FA in fronto-parietal SLF; higher MD, $\lambda_{//}$ and $\lambda_{\perp}$ in IFOF and ILF. No statistically significant difference was found for each of the corresponding fasciculi in the left hemisphere (Fig. 4). Finally, the patient showed higher MD, $\lambda_{//}$ and $\lambda_{\perp}$ in CC (Table 2). No difference was found in the number of tract streamlines comparing the patient with the controls (Table 2). To visually explore the topographical distribution of microstructural damage in each pathway, WM tracts were rendered as maps of FA values for both hemispheres on the high-resolution T1-weighted images of the PCA patient, as showed in Fig. 4.

3.3. VBM study

VBM results are shown in Fig. 5 and Table 3. When compared to controls, PCA patient showed GM atrophy centered on posterior brain regions, involving occipital, parietal and posterior temporal regions, bilaterally. In particular, parietal GM loss involved the entire region, with the superior (right -> left) and inferior parietal lobule (right > left) reaching a corrected level of significance ($p < .05$ family wise error (FWE)). GM loss ($p < .05$ FWE) occurred bilaterally in the superior (left > right) and inferior occipital gyri and cuneus, and in the lingual gyri (right > left). Atrophy also occurred in the right thalamus ($p < .05$ FWE). At $p < .001$ uncorrected, the patients also showed atrophy of the calcarine cortex, precuneus, middle occipital (left > right), and fusiform gyri (left > right), hippocampus, post-central gyrus and the supplementary motor area, bilaterally.

3.4. Segmentation of the hippocampus

Hippocampal volume was similar in the left (2.103 cm^3) and right (2.209 cm^3) hemispheres.

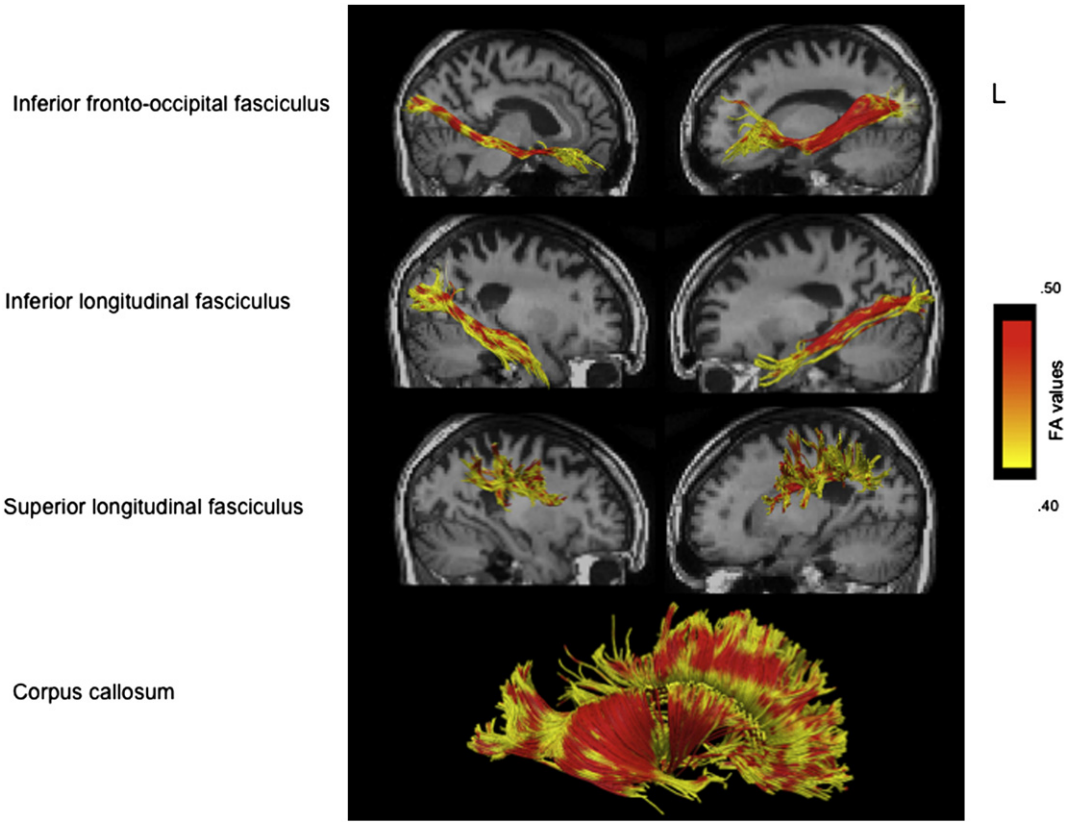

Fig. 4 – WM tracts are rendered as maps of FA for both hemispheres on the coregistered high-resolution T1-weighted images of the PCA patient. FA values are represented in a yellow-to-red color scale where yellow corresponds to lower values and dark red to higher values. Maximum damage is present in the right F-P SLF. Note the loss of fibers in the posterior part of CC.

4. Discussion

Neurodegenerative diseases are likely to progress along functionally and anatomically defined large-scale brain networks. These circuits may become the targets of specific neurodegenerative disorders (Seeley et al., 2009), consistent with the notion of selective vulnerability of anatomo-functional networks in neurodegenerative conditions (Mesulam, 2009). Long-range projections within functional neural circuits may thus play a critical role in brain–behavior relationships.

We studied a 58-year-old patient with PCA and relatively short disease duration. Clinical, cognitive and anatomical features of this patient indicate a predominantly right-hemisphere dysfunction resulting in the impairment of several visuo-spatial functions. The sparing of all the explored fasciculi in the left hemisphere, despite the cortical involvement of the occipital and parietal lobes, is consistent with the cognitive profile, with relatively intact language and calculation abilities.

Visuo-spatial deficits characterized the patient's disease history since its onset. They caused repeated driving accidents involving the left side of the car, probably resulting from visual neglect, which may thus be considered the onset symptom in this case. Optic ataxia was well identified both clinically and by using a computerized touch-screen test, and the deficit was found to be worse for the targets presented on left visual field, in agreement with a lateralized pattern of both GM and WM damage more severe in the right hemisphere. Concerning optic ataxia, our patient showed a hand effect (impaired performance with the right hand in both hemispaces), which might in principle suggest left parietal dysfunction (Perenin and Vighetto, 1988). Unfortunately, a major left-hand apraxia prevented us from testing optic ataxia with the left hand. However, we also note that performance substantially more impaired in the left hemifield than in the right-sided one, with significantly larger distance errors in pointing to left-sided detected targets as compared to right-sided targets (see Fig. 3B). This difference in pointing errors, at variance with left omissions, cannot be explained by left neglect, because it is well known that neglect doubly dissociates from optic ataxia (Perenin and Vighetto, 1988). Thus, although left parietal dysfunction may well have contributed to optic ataxia in this patient, the available evidence indicates a major role of damage to right-hemisphere structures. Anatomical correlates of neglect and optic ataxia may involve adjacent but non-overlapping fronto-parietal networks (Rizzolatti and Matelli, 2003). The posterior nodes of the networks typically damaged in neglect include the inferior parietal lobule and temporo-parietal junction (Thiebaut de Schotten et al., 2005; He et al., 2007), whereas optic ataxia is

Table 2 – DT MRI-derived metrics for WM tracts in the PCA patient and in healthy controls.

			Patient mean	Controls mean (SD)
ILF	L	MD	.80	.79 (.04)
		FA	.47	.44 (.02)
		$\lambda_{//}$	1.20	1.22 (.04)
		$\lambda_{\perp}$	.58	.59 (.04)
		Streamlines (*n*)	115	338 (195.4)
	R	MD	.89#	.77 (.04)
		FA	.40	.43 (.02)
		$\lambda_{//}$	1.30#	1.15 (.08)
		$\lambda_{\perp}$	.68#	.58 (.04)
		Streamlines (*n*)	171	471 (331.5)
IFOF	L	MD	.76	.77 (.02)
		FA	.44	.43 (.02)
		$\lambda_{//}$	1.20	1.13 (.05)
		$\lambda_{\perp}$	.53	.57 (.02)
		Streamlines (*n*)	249	291 (263.9)
	R	MD	.89*	.78 (.02)
		FA	.44	.44 (.01)
		$\lambda_{//}$	1.30*	1.16 (.05)
		$\lambda_{\perp}$	.66*	.57 (.02)
		Streamlines (*n*)	114	379 (148.3)
F-P SLF	L	MD	.73	.70 (.02)
		FA	.44	.43 (.01)
		$\lambda_{//}$	1.10	1.03 (.05)
		$\lambda_{\perp}$	.53	.53 (.03)
		Streamlines (*n*)	690	737 (291.3)
	R	MD	.83#	.74 (.03)
		FA	.38*	.43 (.01)
		$\lambda_{//}$	1.20*	1.06 (.05)
		$\lambda_{\perp}$	.63**	.56 (.01)
		Streamlines (*n*)	727	827 (173)
ARC	L	MD	.75	.71 (.02)
		FA	.46	.46 (.01)
		$\lambda_{//}$	1.10	1.10 (.1)
		$\lambda_{\perp}$	.54	.52 (.02)
		Streamlines (*n*)	390	232 (115)
CC		MD	.89#	.79 (.03)
		FA	.55	.52 (.01)
		$\lambda_{//}$	1.50*	1.31 (.04)
		$\lambda_{\perp}$	.58*	.53 (.02)
		Streamlines (*n*)	3618	4654 (759.1)

*$p < .05$; **$p < .005$; #$p < .001$.
MD, $\lambda_{//}$ and $\lambda_{\perp}$ values are $\times 10^{-3}$ mm^2 sec^{-1}. *p Values refer to the significance test for comparing an individual case with small control samples (Crawford and Garthwaite, 2002).
Abbreviations: L = left; $\lambda_{//}$ = parallel diffusivity; $\lambda_{\perp}$ = transverse diffusivity; *n* = number; R = right; ARC = arcuate.

supposed to correlate with more dorsal and medial parietal damage, even if the specific cortical areas are still debated. Fronto-parietal connections labeled as SLF are structured in different branches (Schmahmann and Pandya, 2006). SLF branches are anatomically and functionally described, run between contiguous but distinct areas of parietal and frontal lobes, and are involved in visuo-spatial (Bartolomeo et al., 2007; Doricchi et al., 2008; Urbanski et al., 2011) and visuo-motor functions (Rizzolatti and Matelli, 2003). The patient's pattern of performance and the massive SLF damage demonstrated by tractography suggest severe and extensive damage to parieto-frontal circuitries. Given the complexity of the neural correlates of visual neglect (Bartolomeo, 2007; Doricchi et al., 2008), callosal damage (Tomaiuolo et al., 2010) or right IFOF damage (Urbanski et al., 2008), both present in this patient, may also have contributed to neglect-related deficits.

In recent years, a debate emerged on whether optic ataxia results from superior or inferior occipito-parietal damage. Perenin (1997) and Coulthard et al. (2006) found that damage to the lateral superior posterior parietal regions and precuneus resulted in optic ataxia. Conversely, Karnath and Perenin (2005) found maximum lesion overlaps bilaterally in the inferior parietal lobes, in the superior parietal lobe but only in the left hemisphere, and in the precuneus. In a meta-analysis of the functional imaging of reaching in healthy subjects, Blangero et al. (2009), identified four main regions: parieto-occipital junction, posterior intraparietal sulcus, mid-intraparietal sulcus region and anterior intraparietal sulcus region. Pisella et al. (2009) suggested the bilateral involvement of superior parietal regions in visuo-motor reaching. Finally, Shallice et al. (2010) identified damage to bilateral lateral and medial superior posterior parietal regions as crucial for optic ataxia in a tumor patient series. Our patient showed a pattern of damage in superior and medial GM parietal regions. Specifically, the parietal cluster atrophy ranged from x 55 to 24, y −65 to −25, z 48 to 57 in the right hemisphere and from x −60 to −15, y −82 to −10, z 19 to 78 in the left hemisphere. These regions correspond to the superior and medial parietal cortex. Our lowest z co-ordinates (outside of superior parietal areas) referred to small atrophy foci in the medial surface (z 25 and z 30) or in more anterior left intraparietal sulcus (z 19 and z 26). These results are consistent with the hypothesis of a role of superior parietal damage in optic ataxia. Concerning the WM, unfortunately, we could not track the higher component of SLF (which might well be implicated in visuo-motor control), because of the limitations of diffusion tensor Imaging (DTI)-based tractography analysis (see the paragraph of limitations below).

Our patient also showed severe left ideomotor apraxia, potentially correlated with both left parietal atrophy and callosal damage. Liepmann was the first to argue that a lesion of the CC, disconnecting the right hemisphere from the left, may lead to unilateral left-hand apraxia (Goldenberg, 2003). Consistent with the presence of a callosal disconnection, our patient also had mild tactile anomia; moreover, she performed better with actual objects than upon verbal command (Heilman and Watson, 2008).

Impaired episodic visual memory, with relatively normal verbal memory, likely resulted from damage to the networks linked by the right ILF, which connects occipital to lateral and medial anterior temporal regions (Shinoura et al., 2007). Consistent with this hypothesis, hippocampal volumes were equivalent in the left and right medial temporal structures, traditionally ascribed to manage respectively verbal and visuo-spatial episodic memory.

The pattern of DT MRI changes suggested that WM damage was likely to reflect the concomitant presence of axonal and myelin pathology, because both $\lambda_{//}$ and $\lambda_{\perp}$ diffusivities values

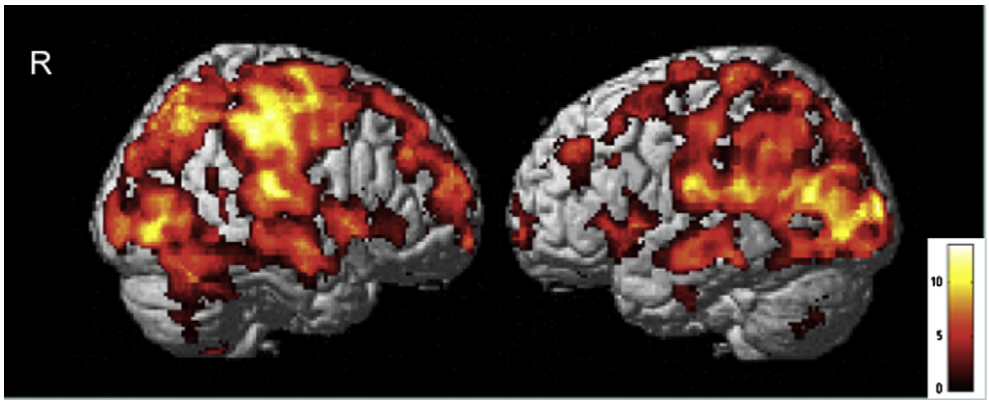

Fig. 5 – VBM results for the patient's scan compared to controls. Regions of GM atrophy are shown on the 3-dimensional rendering of the MNI standard brain. Results are shown at a threshold of $p < .001$ uncorrected.

Table 3 – VBM results for patient's scan compared to 15 age-matched controls.

Brain area		Co-ordinates	Z score
Superior occipital gyrus/cuneus*	R	13 −79 27	5.08
	L	−17 −94 12	5.18
Middle occipital gyrus	R	30 −73 39	4.74
	L	−17 −95 12	5.18
Inferior occipital gyrus*	R	34 −80 −6	5.17
	L	−35 −74 −11	4.32
Calcarine cortex	R	11 −79 1	4.55
	L	−13 −39 7	4.07
Lingual gyrus*	R	16 −67 −4	5.68
	L	−25 −81 −13	4.06
Superior parietal lobe*	R	24 −65 57	5.21
	L	−23 −49 59	4.72
Inferior parietal lobe*	R	42 −57 50	4.65
	L	−26 −47 53	4.17
Precuneus	R	11 −69 41	5.16
	L	−13 −60 37	4.43
Fusiform gyrus	R	24 −55 −11	4.65
	L	−26 −46 −15	4.89
Superior temporal gyrus	R	50 −25 14	4.89
	L	−56 −39 12	4.55
Middle temporal gyrus	R	52 −75 1	4.47
	L	−51 −66 14	5.08
Inferior temporal gyrus	R	42 −55 −75	4.04
	L	−52 −59 −6	4.09
Hippocampus	R	18 −34 3	4.61
	L	−13 −67 19	4.10
Thalamus*	R	19 −26 7	5.59
	L	−11 −26 7	4.55
Post-central gyrus	R	55 −25 48	5.52
	L	−23 −47 55	5.46
Supplementary motor area	R	15 −7 64	4.42
	L	−13 −7 68	4.23

All results are shown at the threshold of $p < .001$ uncorrected, * indicates those clusters that survived the correction for multiple comparisons ($p < .05$). Abbreviations: L = left; R = right.

were increased in the patient compared to controls, for all right-sided fasciculi, as well as for the CC. The presence of myelinic damage in addition to axonal damage, along with evidence of an underlying AD pathology suggested by altered values in the CSF, highlights the importance of WM damage in neurodegenerative conditions, conventionally ascribed to an isolated cortical GM involvement. It is common knowledge that PCA is associated with occipito-parietal GM atrophy, but evidence concerning microstructural WM damage obtained through DTI-based tractography is scanty. Recently, WM pathology has been proposed to play an important role in the onset and progression of AD. According to the so-called retrogenesis model (see Stricker et al., 2009), WM degeneration tends to be more severe in cerebral regions with late myelination in the course of brain development, such as the neocortical long-range association fibers. Although the retrogenesis model emphasizes the role of myelin breakdown, possible contributions from Wallerian degeneration to WM changes in degenerative dementia cannot be ruled out given the nature of the disease. It is usually assumed that the degree of myelination modulates the radial diffusivity, which is pathologically increased for the tracts of interest in our patient. However, we cannot exclude the effect of other plausible biological and physical phenomena such as fiber reorganization, destruction of intracellular compartments and glial alterations that can also modify the radial diffusivity (Beaulieu, 2002).

Supporting evidence of WM damage in AD comes from *in vivo* imaging studies (Zhang et al., 2009; Damoiseaux et al., 2009; Stricker et al., 2009; Pievani et al., 2010), as well as from pathological series (Brun and Englund, 1986; Englund et al., 1988; Englund and Brun, 1990; Englund, 1998; Bronge et al., 2002; Sjobeck et al., 2003; Sjobeck and Englund, 2003). However, as mentioned in the introduction, only two DTI-based single case studies are currently available on PCA (Duning et al., 2009; Yoshida et al., 2004), neither of which used the most recent tractography analysis methods.

There are some limitations in our tractography analysis, since the tensor-based algorithm we used does not show crossing or fanning fibers (McNab et al., 2009), likely underestimating the disconnection. Other methods are more apt to show tracts running close to the cortical surface, such as the

most dorsal branch of the SLF (Thiebaut de Schotten et al., 2011). Moreover, the reconstruction could miss the tracts with greater damage and with lower FA, because of difficulties in visualizing and measuring the most affected streamlines. Future approach will need to use new algorithms reconstructing the complex organization of the WM fibers (Dell'Acqua et al., 2007) and estimating the fiber orientation in damaged brain (Dell'Acqua et al., 2010).

In conclusion, cognitive and anatomical data in this patient indicate a relatively selective impairment of large-scale fronto-parietal and fronto-temporal networks in the right hemisphere, resulting from both GM and WM damage, and combined with a relative sparing of left-lateralized pathways. These network-based dysfunctions can account for the peculiar combination of impaired and spared visuo-spatial/language domains that is typical of PCA and rarely observed in other neurodegenerative diseases.

Acknowledgments

We thank our patient Dr. B.N. for her willingness, will-power, and interest in our research. We also thank Bastien Oliveiro, Sophie Ferrieux and Elisabetta Pagani for their useful support. The authors acknowledge the support of the French Agence Nationale de la Recherche (ANR-07-LVIE-002-01 – Biomage study). Dr. Migliaccio was funded by the Neuropole de Recherche Francilien (NeRF) and the European Neurological Society (ENS).

REFERENCES

Agosta F, Henry RG, Migliaccio R, Neuhaus J, Miller BL, Dronkers NF, et al. Language networks in semantic dementia. *Brain*, 133(Pt 1): 286–299, 2010.

Alladi S, Xuereb J, Bak T, Nestor P, Knibb J, Patterson K, et al. Focal cortical presentations of Alzheimer's disease. *Brain*, 130(Pt 10): 2636–2645, 2007.

Andrade K, Samri D, Sarazin M, de Souza LC, Cohen L, de Schotten MT, et al. Visual neglect in posterior cortical atrophy. *BMC Neurology*, 10: 68, 2010.

Ashburner J. A fast diffeomorphic image registration algorithm. *NeuroImage*, 38(1): 95–113, 2007.

Azouvi P, Bartolomeo P, Beis JM, Perennou D, Pradat-Diehl P, and Rousseaux M. A battery of tests for the quantitative assessment of unilateral neglect. *Restorative Neurology and Neuroscience*, 24(4–6): 273–285, 2006.

Bartolomeo P. Visual neglect. *Current Opinion in Neurology*, 20(4): 381–386, 2007.

Bartolomeo P. The quest for the 'critical lesion site' in cognitive deficits: Problems and perspectives. *Cortex*, 47(8): 1010–1012, 2011.

Bartolomeo P, Thiebaut de Schotten M, and Doricchi F. Left unilateral neglect as a disconnection syndrome. *Cerebral Cortex*, 17(11): 2479–2490, 2007.

Beaulieu C. The basis of anisotropic water diffusion in the nervous system – a technical review. *NMR in Biomedicine*, 15(7–8): 435–455, 2002.

Benson DF, Davis RJ, and Snyder BD. Posterior cortical atrophy. *Archives of Neurology*, 45(7): 789–793, 1988.

Blangero A, Menz MM, McNamara A, and Binkofski F. Parietal modules for reaching. *Neuropsychologia*, 47(6): 1500–1507, 2009.

Bokde AL, Teipel SJ, Drzezga A, Thissen J, Bartenstein P, Dong W, et al. Association between cognitive performance and cortical glucose metabolism in patients with mild Alzheimer's disease. *Dementia and Geriatric Cognitive Disorders*, 20(6): 352–357, 2005.

Bronge L, Bogdanovic N, and Wahlund LO. Postmortem MRI and histopathology of white matter changes in Alzheimer brains. A quantitative, comparative study. *Dementia and Geriatric Cognitive Disorders*, 13(4): 205–212, 2002.

Brun A and Englund E. A white matter disorder in dementia of the Alzheimer type: A pathoanatomical study. *Annals of Neurology*, 19(3): 253–262, 1986.

Catani M, Allin MP, Husain M, Pugliese L, Mesulam MM, Murray RM, et al. Symmetries in human brain language pathways correlate with verbal recall. *Proceedings of the National Academy of Sciences USA*, 104(43): 17163–17168, 2007.

Catani M and ffytche DH. The rises and falls of disconnection syndromes. *Brain*, 128(Pt 10): 2224–2239, 2005.

Catani M and Thiebaut de Schotten M. A diffusion tensor imaging tractography atlas for virtual in vivo dissections. *Cortex*, 44(8): 1105–1132, 2008.

Chupin M, Gerardin E, Cuingnet R, Boutet C, Lemieux L, Lehericy S, et al. Fully automatic hippocampus segmentation and classification in Alzheimer's disease and mild cognitive impairment applied on data from ADNI. *Hippocampus*, 19(6): 579–587, 2009.

Coulthard E, Parton A, and Husain M. Action control in visual neglect. *Neuropsychologia*, 44(13): 2717–2733, 2006.

Crawford JR and Garthwaite PH. Investigation of the single case in neuropsychology: Confidence limits on the abnormality of test scores and test score differences. *Neuropsychologia*, 40(8): 1196–1208, 2002.

Damoiseaux JS, Smith SM, Witter MP, Sanz-Arigita EJ, Barkhof F, Scheltens P, et al. White matter tract integrity in aging and Alzheimer's disease. *Human Brain Mapping*, 30(4): 1051–1059, 2009.

de Souza LC, Corlier F, Habert MO, Uspenskaya O, Maroy R, Lamari F, et al. Similar amyloid-beta burden in posterior cortical atrophy and Alzheimer's disease. *Brain*, 134(Pt 7): 2036–2043, 2011.

Dell'Acqua F, Rizzo G, Scifo P, Clarke RA, Scotti G, and Fazio F. A model-based deconvolution approach to solve fiber crossing in diffusion-weighted MR imaging. *IEEE Transactions on Biomedical Engineering*, 54(3): 462–472, 2007.

Dell'Acqua F, Scifo P, Rizzo G, Catani M, Simmons A, Scotti G, et al. A modified damped Richardson–Lucy algorithm to reduce isotropic background effects in spherical deconvolution. *NeuroImage*, 49(2): 1446–1458, 2010.

Doricchi F, Thiebaut de Schotten M, Tomaiuolo F, and Bartolomeo P. White matter (dis)connections and gray matter (dys)functions in visual neglect: Gaining insights into the brain networks of spatial awareness. *Cortex*, 44(8): 983–995, 2008.

Duning T, Warnecke T, Mohammadi S, Lohmann H, Schiffbauer H, Kugel H, et al. Pattern and progression of white-matter changes in a case of posterior cortical atrophy using diffusion tensor imaging. *Journal of Neurology, Neurosurgery & Psychiatry*, 80(4): 432–436, 2009.

Englund E. Neuropathology of white matter changes in Alzheimer's disease and vascular dementia. *Dementia and Geriatric Cognitive Disorders*, 9(Suppl. 1): 6–12, 1998.

Englund E and Brun A. White matter changes in dementia of Alzheimer's type: The difference in vulnerability between cell compartments. *Histopathology*, 16(5): 433–439, 1990.

Englund E, Brun A, and Alling C. White matter changes in dementia of Alzheimer's type. Biochemical and neuropathological correlates. *Brain*, 111(Pt 6): 1425–1439, 1988.

Freedman L, Selchen DH, Black SE, Kaplan R, Garnett ES, and Nahmias C. Posterior cortical dementia with alexia:

Neurobehavioural, MRI, and PET findings. *Journal of Neurology, Neurosurgery & Psychiatry*, 54(5): 443–448, 1991.
Frisoni GB, Pievani M, Testa C, Sabattoli F, Bresciani L, Bonetti M, et al. The topography of grey matter involvement in early and late onset Alzheimer's disease. *Brain*, 130(Pt 3): 720–730, 2007.
Galton CJ, Patterson K, Xuereb JH, and Hodges JR. Atypical and typical presentations of Alzheimer's disease: A clinical, neuropsychological, neuroimaging and pathological study of 13 cases. *Brain*, 123(Pt 3): 484–498, 2000.
Goldenberg G. Apraxia and beyond: Life and work of Hugo Liepmann. *Cortex*, 39(3): 509–524, 2003.
Gorno-Tempini ML, Murray RC, Rankin KP, Weiner MW, and Miller BL. Clinical, cognitive and anatomical evolution from nonfluent progressive aphasia to corticobasal syndrome: A case report. *Neurocase*, 10(6): 426–436, 2004.
He BJ, Snyder AZ, Vincent JL, Epstein A, Shulman GL, and Corbetta M. Breakdown of functional connectivity in frontoparietal networks underlies behavioral deficits in spatial neglect. *Neuron*, 53(6): 905–918, 2007.
Heilman KM and Watson RT. The disconnection apraxias. *Cortex*, 44(8): 975–982, 2008.
Jackson SR, Newport R, Mort D, and Husain M. Where the eye looks, the hand follows; limb-dependent magnetic misreaching in optic ataxia. *Current Biology*, 15(1): 42–46, 2005.
Karnath HO and Perenin MT. Cortical control of visually guided reaching: Evidence from patients with optic ataxia. *Cerebral Cortex*, 15(10): 1561–1569, 2005.
Kas A, de Souza LC, Samri D, Bartolomeo P, Lacomblez L, Kalafat M, et al. Neural correlates of cognitive impairment in posterior cortical atrophy. *Brain*, 134(Pt 5): 1464–1478, 2011.
Kravitz DJ, Saleem KS, Baker CI, and Mishkin M. A new neural framework for visuospatial processing. *Nature Reviews Neuroscience*, 12(4): 217–230, 2011.
Lehmann M, Barnes J, Ridgway GR, Wattam-Bell J, Warrington EK, Fox NC, et al. Basic visual function and cortical thickness patterns in posterior cortical atrophy. *Cerebral Cortex*, 21(9): 2122–2132, 2011.
McMonagle P, Deering F, Berliner Y, and Kertesz A. The cognitive profile of posterior cortical atrophy. *Neurology*, 66(3): 331–338, 2006.
McNab JA, Jbabdi S, Deoni SC, Douaud G, Behrens TE, and Miller KL. High resolution diffusion-weighted imaging in fixed human brain using diffusion-weighted steady state free precession. *NeuroImage*, 46(3): 775–785, 2009.
Mendez MF, Ghajarania M, and Perryman KM. Posterior cortical atrophy: Clinical characteristics and differences compared to Alzheimer's disease. *Dementia and Geriatric Cognitive Disorders*, 14(1): 33–40, 2002.
Mesulam M. Defining neurocognitive networks in the BOLD new world of computed connectivity. *Neuron*, 62(1): 1–3, 2009.
Migliaccio R, Agosta F, Rascovsky K, Karydas A, Bonasera S, Rabinovici GD, et al. Clinical syndromes associated with posterior atrophy: Early age at onset AD spectrum. *Neurology*, 73(19): 1571–1578, 2009.
Nestor PJ, Caine D, Fryer TD, Clarke J, and Hodges JR. The topography of metabolic deficits in posterior cortical atrophy (the visual variant of Alzheimer's disease) with FDG-PET. *Journal of Neurology, Neurosurgery & Psychiatry*, 74(11): 1521–1529, 2003.
Peigneux P and Van der Linden M. Présentation d'une batterie neuropsychologique et cognitive pour l'évaluation de l'apraxie gestuelle. *Revue de Neuropsychologie*, 10: 311–362, 2000.
Perenin M-T. Optic ataxia and unilateral neglect: Clinical evidence for dissociable spatial functions in posterior parietal cortex. In Karnath H-O and Thier P (Eds), *Parietal Lobe Contributions to Orientation in 3D Space*. Berlin: Springer, 1997: 289–308.
Perenin MT and Vighetto A. Optic ataxia: A specific disruption in visuomotor mechanisms. I. Different aspects of the deficit in reaching for objects. *Brain*, 111(Pt 3): 643–674, 1988.
Pierpaoli C, Barnett A, Pajevic S, Chen R, Penix LR, Virta A, et al. Water diffusion changes in Wallerian degeneration and their dependence on white matter architecture. *NeuroImage*, 13(6 Pt 1): 1174–1185, 2001.
Pievani M, Agosta F, Pagani E, Canu E, Sala S, Absinta M, et al. Assessment of white matter tract damage in mild cognitive impairment and Alzheimer's disease. *Human Brain Mapping*, 31(12): 1862–1875, 2010.
Pisella L, Ota H, Vighetto A, and Rossetti Y. Optic ataxia and Balint's syndrome: Neuropsychological and neurophysiological prospects. *Handbook of Clinical Neurology*, 88: 393–415, 2008.
Pisella L, Sergio L, Blangero A, Torchin H, Vighetto A, and Rossetti Y. Optic ataxia and the function of the dorsal stream: Contributions to perception and action. *Neuropsychologia*, 47(14): 3033–3044, 2009.
Rabinovici GD, Furst AJ, Alkalay A, Racine CA, O'Neil JP, Janabi M, et al. Increased metabolic vulnerability in early-onset Alzheimer's disease is not related to amyloid burden. *Brain*, 133(Pt 2): 512–528, 2010.
Renner JA, Burns JM, Hou CE, McKeel Jr DW, Storandt M, and Morris JC. Progressive posterior cortical dysfunction: A clinicopathologic series. *Neurology*, 63(7): 1175–1180, 2004.
Rizzolatti G and Matelli M. Two different streams form the dorsal visual system: Anatomy and functions. *Experimental Brain Research*, 153(2): 146–157, 2003.
Rosenbloom MH, Alkalay A, Agarwal N, Baker SL, O'Neil JP, Janabi M, et al. Distinct clinical and metabolic deficits in PCA and AD are not related to amyloid distribution. *Neurology*, 76(21): 1789–1796, 2011.
Schmahmann JD and Pandya DN. *Fiber Pathways of the Brain*. Oxford University Press, 2006.
Schmidtke K, Hull M, and Talazko J. Posterior cortical atrophy: Variant of Alzheimer's disease? A case series with PET findings. *Journal of Neurology*, 252(1): 27–35, 2005.
Seeley WW, Crawford RK, Zhou J, Miller BL, and Greicius MD. Neurodegenerative diseases target large-scale human brain networks. *Neuron*, 62(1): 42–52, 2009.
Shallice T, Mussoni A, D'Agostino S, and Skrap M. Right posterior cortical functions in a tumour patient series. *Cortex*, 46(9): 1178–1188, 2010.
Shinoura N, Suzuki Y, Tsukada M, Katsuki S, Yamada R, Tabei Y, et al. Impairment of inferior longitudinal fasciculus plays a role in visual memory disturbance. *Neurocase*, 13(2): 127–130, 2007.
Sjobeck M and Englund E. Glial levels determine severity of white matter disease in Alzheimer's disease: A neuropathological study of glial changes. *Neuropathology and Applied Neurobiology*, 29(2): 159–169, 2003.
Sjobeck M, Haglund M, Persson A, Sturesson K, and Englund E. Brain tissue microarrays in dementia research: White matter microvascular pathology in Alzheimer's disease. *Neuropathology*, 23(4): 290–295, 2003.
Stricker NH, Schweinsburg BC, Delano-Wood L, Wierenga CE, Bangen KJ, Haaland KY, et al. Decreased white matter integrity in late-myelinating fiber pathways in Alzheimer's disease supports retrogenesis. *NeuroImage*, 45(1): 10–16, 2009.
Tang-Wai DF, Graff-Radford NR, Boeve BF, Dickson DW, Parisi JE, Crook R, et al. Clinical, genetic, and neuropathologic characteristics of posterior cortical atrophy. *Neurology*, 63(7): 1168–1174, 2004.
Thiebaut de Schotten M, Dell'Acqua F, Forkel S, Simmons A, Vergani F, Murphy DGM, et al. Lateralized brain network for visuo-spatial attention. *Nature Precedings*, 2011.

Thiebaut de Schotten M, Urbanski M, Duffau H, Volle E, Levy R, Dubois B, et al. Direct evidence for a parietal–frontal pathway subserving spatial awareness in humans. *Science*, 309(5744): 2226–2228, 2005.

Tomaiuolo F, Voci L, Bresci M, Cozza S, Posteraro F, Oliva M, et al. Selective visual neglect in right brain damaged patients with splenial interhemispheric disconnection. *Experimental Brain Research*, 206(2): 209–217, 2010.

Ungerleider L and Mishkin M. Two cortical visual systems. In Ingle DJ, Goodale MA, and Mansfield RJW (Eds), *Analysis of Motor Behavior*. Cambridge: MIT Press, 1982: 549–586.

Urbanski M, Thiebaut de Schotten M, Rodrigo S, Catani M, Oppenheim C, Touze E, et al. Brain networks of spatial awareness: Evidence from diffusion tensor imaging tractography. *Journal of Neurology, Neurosurgery & Psychiatry*, 79(5): 598–601, 2008.

Urbanski M, Thiebaut de Schotten M, Rodrigo S, Oppenheim C, Touzé E, Méder JF, et al. DTI-MR tractography of white matter damage in stroke patients with neglect. *Experimental Brain Research*, 208(4): 491–505, 2011.

von Gunten A, Bouras C, Kovari E, Giannakopoulos P, and Hof PR. Neural substrates of cognitive and behavioral deficits in atypical Alzheimer's disease. *Brain Research Reviews*, 51(2): 176–211, 2006.

Wedeen VJ, Wang RP, Schmahmann JD, Benner T, Tseng WY, Dai G, et al. Diffusion spectrum magnetic resonance imaging (DSI) tractography of crossing fibers. *NeuroImage*, 41(4): 1267–1277, 2008.

Whitwell JL, Jack Jr CR, Kantarci K, Weigand SD, Boeve BF, Knopman DS, et al. Imaging correlates of posterior cortical atrophy. *Neurobiology of Aging*, 28(7): 1051–1061, 2007.

Yasuno F, Imamura T, Hirono N, Ishii K, Sasaki M, Ikejiri Y, et al. Age at onset and regional cerebral glucose metabolism in Alzheimer's disease. *Dementia and Geriatric Cognitive Disorders*, 9(2): 63–67, 1998.

Yoshida T, Shiga K, Yoshikawa K, Yamada K, and Nakagawa M. White matter loss in the splenium of the corpus callosum in a case of posterior cortical atrophy: A diffusion tensor imaging study. *European Neurology*, 52(2): 77–81, 2004.

Zhang Y, Schuff N, Du AT, Rosen HJ, Kramer JH, Gorno-Tempini ML, et al. White matter damage in frontotemporal dementia and Alzheimer's disease measured by diffusion MRI. *Brain*, 132(Pt 9): 2579–2592, 2009.